MONOCLONAL ANTIBODIES IN IMMUNODIAGNOSIS AND IMMUNOTHERAPY
Volume XX, Number XX, 2022

DOI: 10.1089/mab.2021.0058

Development of Monoclonal Antibody 281-mG$_{2a}$-f Against Golden Hamster Podoplanin

Ren Nanamiya,[1] Hiroyuki Suzuki,[2] Junko Takei,[1,3] Guanjie Li,[2] Nohara Goto,[2,4] Hiroyuki Harada,[3] Masaki Saito,[2] Tomohiro Tanaka,[1] Teizo Asano,[1] Mika K. Kaneko,[1] and Yukinari Kato[1,2]

Golden (Syrian) hamster (*Mesocricetus auratus*) is a small animal model of severe acute respiratory syndrome coronavirus 2 (SARS-CoV-2) infections. Pathological analyses of the tissues are required to understand the pathogenesis of SARS-CoV-2 and the evaluation of therapeutic modalities, including neutralizing monoclonal antibodies (mAbs). However, mAbs that recognize the golden hamster-derived antigens and distinguish specific cell types, such as the pneumocytes, are limited. Podoplanin (PDPN) is an essential marker of lung type I alveolar epithelial cells, kidney podocytes, and lymphatic endothelial cells. In this study, an anti-Chinese hamster (*Cricetulus griseus*) PDPN mAb PMab-281 (IgG_3, kappa) was established using the Cell-Based Immunization and Screening (CBIS) method. A defucosylated mouse IgG_{2a} version of PMab-281 (281-mG$_{2a}$-f) was also developed. The 281-mG$_{2a}$-f strongly recognized both the Chinese hamster and the golden hamster PDPN using flow cytometry and could detect lung type I alveolar epithelial cells, lymphatic endothelial cells, and Bowman's capsules in the kidney from the golden hamster using immunohistochemistry. These results suggest the usefulness of 281-mG$_{2a}$-f for analyzing the golden hamster-derived tissues and cells for SARS-CoV-2 research.

Keywords: hamster podoplanin, PDPN, monoclonal antibody, CBIS

Introduction

PODOPLANIN (PDPN) is a type I transmembrane mucin-like sialoglycoprotein that has a heavily glycosylated N-terminal extracellular domain, a single transmembrane domain, and a short intracellular domain. PDPN is also named T1α, which is expressed at the apical surface of lung type I alveolar epithelial cells.[1,2] PDPN is expressed in kidney podocytes.[3] Podocytes have foot processes, attach to glomerular capillaries at the glomerular basement membrane and play critical roles as slit diaphragm filtration barriers.[4] PDPN is known as a marker of lymphatic endothelial cells.[5,6] Mice lacking PDPN die at birth due to respiratory defects and have failed in the lymphatic vessel pattern formation.[7] These results show the importance of PDPN in lung epithelium and lymphatic endothelial development.

In animal models of severe acute respiratory syndrome coronavirus 2 (SARS-CoV-2), golden (Syrian) hamsters (*Mesocricetus auratus*) resemble the pathogenesis and transmissibility found in humans with mild SARS-CoV-2 infections. Immunohistochemical analyses showed that the viral antigens in the nasal mucosa, bronchial epithelial cells, and areas of lung consolidation were detected on days two and five after inoculation with SARS-CoV-2. Seven days after inoculation, viral clearance with pneumocyte hyperplasia was observed. Notably, SARS-CoV-2 was transmitted from inoculated hamsters to naive hamsters through direct contact and aerosols.[8] These results propose the usefulness of golden hamsters as a small animal model to understand the host defense in the respiratory tissues and contribute to the evaluation of neutralizing antibodies against SARS-CoV-2 spike proteins.[9] However, there is a limitation of the

[1]Department of Antibody Drug Development, Tohoku University Graduate School of Medicine, Sendai, Japan.
[2]Department of Molecular Pharmacology, Tohoku University Graduate School of Medicine, Sendai, Japan.
[3]Department of Oral and Maxillofacial Surgery, Graduate School of Medical and Dental Sciences, Tokyo Medical and Dental University, Bunkyo-ku, Japan.
[4]Department of Experimental Pathology, Graduate School of Comprehensive Human Sciences, Faculty of Medicine, University of Tsukuba, Tsukuba, Japan.

pathological analysis owing to the lack of antibodies that can recognize the golden hamster-derived antigens and distinguish the specific cells in the lung.

This study aimed to develop anti-hamster PDPN monoclonal antibodies (mAbs), which are useful in immunohistochemistry, using the Cell-Based Immunization and Screening (CBIS) method. CBIS method includes the immunization of antigen-overexpressing cells and the high-throughput hybridoma screening using flow cytometry. Mice were immunized with Chinese hamster ovary (CHO)/Chinese hamster PDPN (ChamPDPN)-overexpressed cells and mAbs was established. Furthermore, whether those mAbs could cross-react with golden hamster PDPN (GhamPDPN) in flow cytometry and immunohistochemistry was investigated.

Materials and Methods

Cell lines

CHO-K1 and mouse multiple myeloma P3X63Ag8U.1 (P3U1) cells were obtained from the American Type Culture Collection (ATCC, Manassas, VA, USA). BHK-21 (golden hamster kidney cell line) was obtained from the Cell Resource Center for Biomedical Research Institute of Development, Aging, and Cancer, Tohoku University (Miyagi, Japan).

ChamPDPN cDNA (Accession No.: AB205160) with N-terminal MAP tag[10,11] or with 2×RIEDL tag[12] was subcloned into a pCAG-Ble vector (FUJIFILM Wako Pure Chemical Corporation, Osaka, Japan). Synthesized DNA (Eurofins Genomics KK) encoding GhamPDPN (Accession No.: XM_021233536) with 2×RIEDL tag was subcloned into a pCAG-Ble vector. Plasmids were transfected using Lipofectamine LTX with Plus Reagent (Thermo Fisher Scientific, Inc., Waltham, MA, USA). Stable transfectants were selected using cell sorter (SH800; Sony Biotechnology Corp., Tokyo, Japan) and were cultivated in media containing 0.5 mg/mL of Zeocin (InvivoGen, San Diego, CA, USA). CHO/MAP-ChamPDPN was subsequently used as an immunogen, while CHO/2×RIEDL-ChamPDPN and CHO/2×RIEDL-GhamPDPN were used for further analyses.

CHO-K1, CHO/MAP-ChamPDPN, CHO/2×RIEDL-ChamPDPN, CHO/2×RIEDL-GhamPDPN, P3U1, and BHK-21 were cultured in Roswell Park Memorial Institute (RPMI) 1640 media (Nacalai Tesque, Inc., Kyoto, Japan) supplemented with 10% heat-inactivated fetal bovine serum (Thermo Fisher Scientific, Inc.), 100 U/mL of penicillin, 100 μg/mL streptomycin, and 0.25 μg/mL amphotericin B (Nacalai Tesque, Inc.), and incubated at 37°C in a humidified atmosphere containing 5% CO_2.

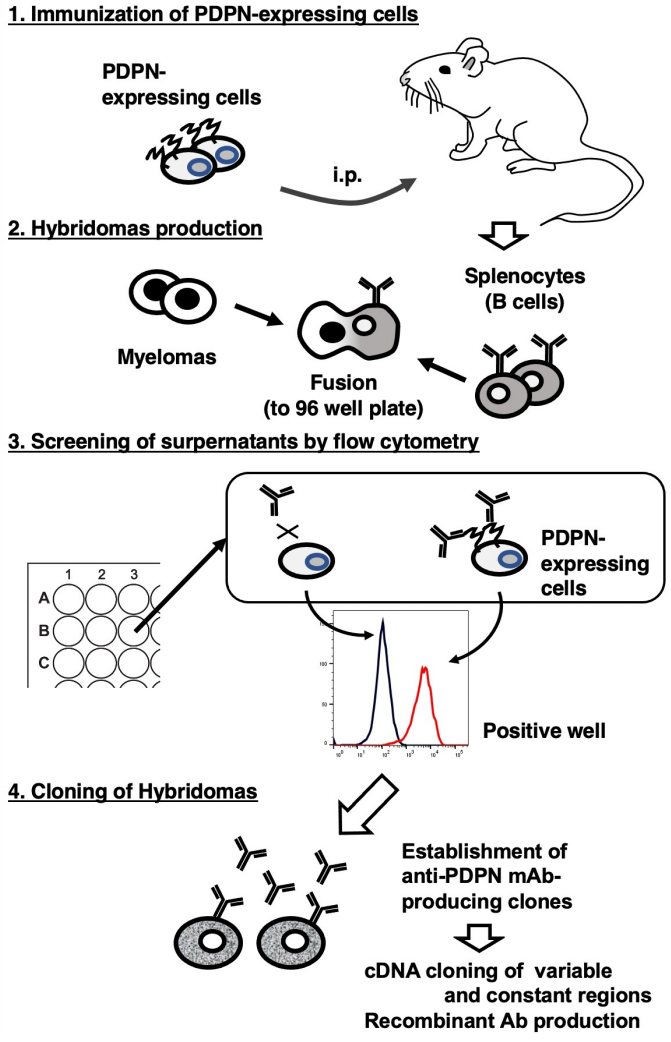

FIG. 1. Schematic procedure of the CBIS method. CHO/ChamPDPN cells were inoculated into the mice intraperitoneally (i.p.). Splenic cells were fused with myeloma cells, and the culture supernatants from hybridomas were screened for anti-ChamPDPN antibody production using flow cytometry. CBIS, Cell-Based Immunization and Screening; ChamPDPN, Chinese hamster PDPN; CHO, Chinese hamster ovary; PDPN, podoplanin.

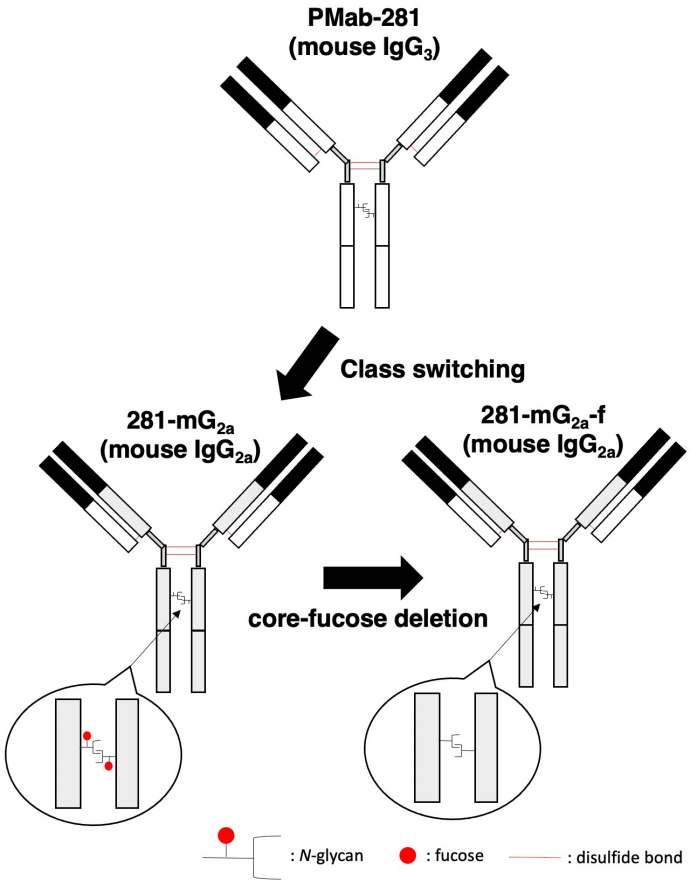

FIG. 2. Production of 281-mG_{2a} (mouse IgG_{2a}) and 281-mG_{2a}-f (defucosylated form) from an anti-PDPN mAb, PMab-281 (mouse IgG_3).

Hybridoma production

Female BALB/c mice (6-week-old) were purchased from CLEA Japan (Tokyo, Japan). The animals were housed under specific pathogen-free conditions. The Animal Care and Use Committee of Tohoku University approved all animal experiments. We used the CBIS method[13–19] to develop mAbs against ChamPDPN. A BALB/c mouse was immunized with CHO/MAP-ChamPDPN cells (1×10^8) intraperitoneally (i.p.) with Imject Alum (Thermo Fisher Scientific, Inc.). The procedure included three additional immunizations with CHO/MAP-ChamPDPN cells (1×10^8) followed by a final booster injection of CHO/MAP-ChamPDPN cells (1×10^8) 2 days before the harvest of splenic cells.

Subsequently, splenic cells were fused with P3U1 cells using polyethylene glycol 1500 (PEG1500; Roche Diagnostics, Indianapolis, IN, USA). The hybridomas were then grown in RPMI 1640 media supplemented with hypoxanthine, aminopterin, and thymidine (HAT) for selection (Thermo Fisher Scientific, Inc.). The culture supernatants were screened for anti-ChamPDPN antibody production using flow cytometry.

Antibodies

To generate 281-mG$_{2a}$, we subcloned V_H cDNA of PMab-281 and C_H of mouse IgG$_{2a}$ into the pCAG-Neo vector, along with cDNA of PMab-281 light chain into the pCAG-Zeo vector, respectively. The vector of 281-mG$_{2a}$ was transfected

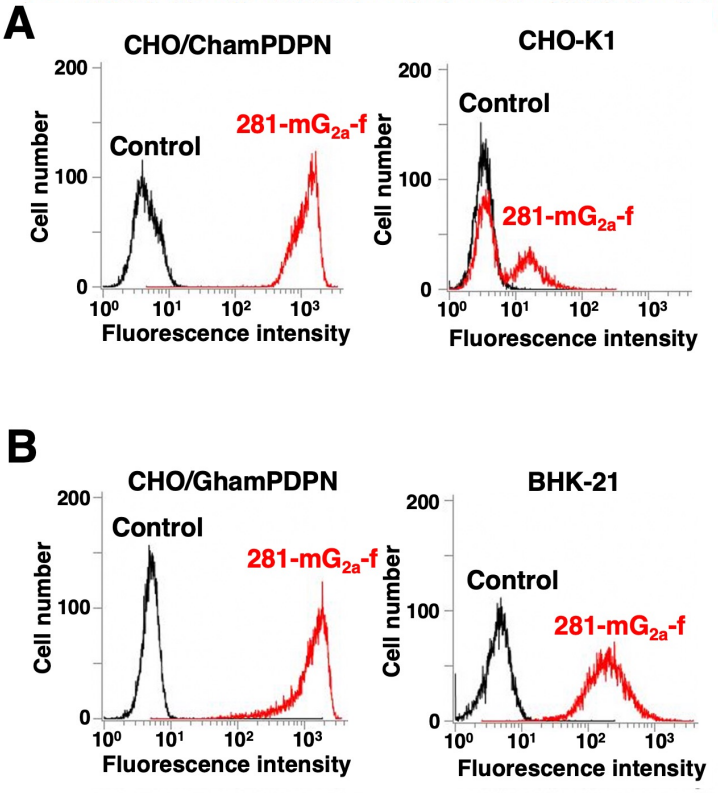

FIG. 3. Flow cytometry using 281-mG$_{2a}$-f. **(A)** CHO/ChamPDPN and CHO-K1 cells were treated with 1 μg/mL of 281-mG$_{2a}$-f, followed by treatment using Alexa Fluor 488-conjugated anti-mouse IgG; black line, negative control. **(B)** CHO/GhamPDPN and BHK-21 cells were treated with 1 μg/mL of 281-mG$_{2a}$-f, followed by treatment using Alexa Fluor 488-conjugated anti-mouse IgG; black line, negative control. GhamPDPN, golden hamster PDPN.

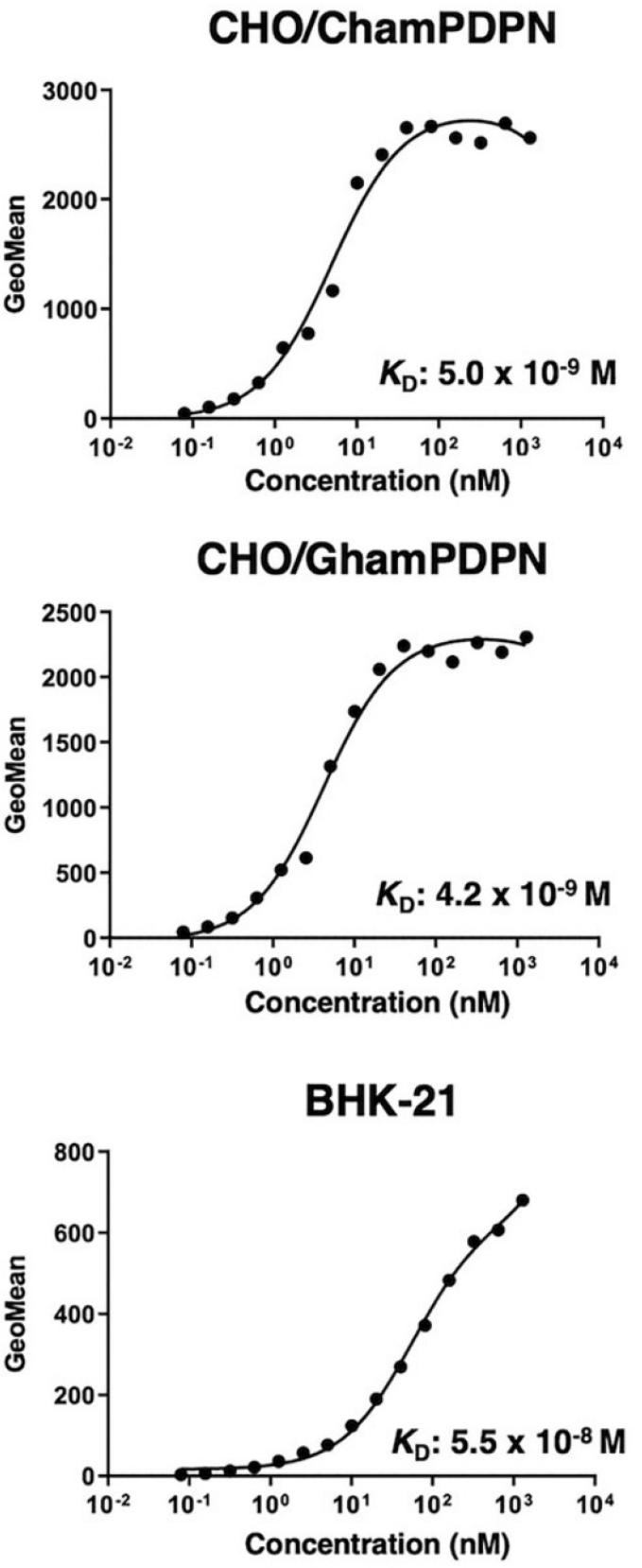

FIG. 4. Determination of the binding affinity of 281-mG$_{2a}$-f. CHO/ChamPDPN (upper), CHO/GhamPDPN (middle), or BHK-21 (bottom) cells were suspended in 100 μL serially diluted 281-mG$_{2a}$-f (100–0.006 μg/mL). Then, Alexa Fluor 488-conjugated anti-mouse IgG was treated. Fluorescence data were obtained using a BD FACSLyric. The dissociation constant (K_D) was calculated by fitting binding isotherms to built-in, one-site binding models in GraphPad PRISM 8.

using the ExpiCHO Expression System (Thermo Fisher Scientific, Inc.). The resulting mAb, 281-mG$_{2a}$-f, was purified with Ab-Capcher (ProteNova, Kagawa, Japan).

Flow cytometry

BHK-21, CHO/2×RIEDL-ChamPDPN, CHO/2×RIEDL-GhamPDPN, and parental CHO-K1 cells (2×10^5 cells/mL) were harvested after a brief exposure to 0.25% trypsin in 1 mM ethylenediaminetetraacetic acid (Nacalai Tesque, Inc.). After washing with 0.1% bovine serum albumin (Nacalai Tesque, Inc.) in phosphate-buffered saline (PBS; Nacalai Tesque, Inc.), cells were treated with 281-mG$_{2a}$-f (1 μg/mL) for 30 minutes at 4°C, followed by Alexa Fluor 488-conjugated anti-mouse IgG (1:1000; Product No. 4408; Cell Signaling Technology, Inc., Danvers, MA, USA). Fluorescence data were collected using the EC800 Cell Analyzer (Sony Biotechnology Corp.).

Determination of the binding affinity

Cells were suspended in 100 μL of serially diluted 281-mG$_{2a}$-f (0.006–100 μg/mL) followed by Alexa Fluor 488-conjugated anti-mouse IgG (1:200; Cell Signaling Technology, Inc.). Fluorescence data were collected using the EC800 Cell Analyzer. The dissociation constant (K_D) was calculated by fitting binding isotherms to built-in one-site binding models in GraphPad Prism 8 (GraphPad Software, Inc., La Jolla, CA, USA).

Immunohistochemical analysis

Normal golden hamster tissues (lung [Cat. No.: AP-601] and kidney [Cat. No.: AP-901]) were purchased from Zyagen (San Diego, CA, USA). Histological sections (4 μm thickness) were autoclaved in citrate buffer (pH 6.0; Nichirei Biosciences, Inc., Tokyo, Japan) for 20 minutes. After blocking with SuperBlock T20 (PBS) Blocking Buffer (Thermo Fisher Scientific, Inc.), sections were incubated with anti-281-mG$_{2a}$-f (1 μg/mL) for 1 hour at room temperature and treated using EnVision+ Kit (Agilent Technologies, Inc.) for 30 minutes. Color was developed using 3,3′-diaminobenzidine tetrahydrochloride (Agilent Technologies, Inc.) for 2 minutes, and counterstaining was performed with Hematoxylin and Eosin (FUJIFILM Wako Pure Chemical Corporation).

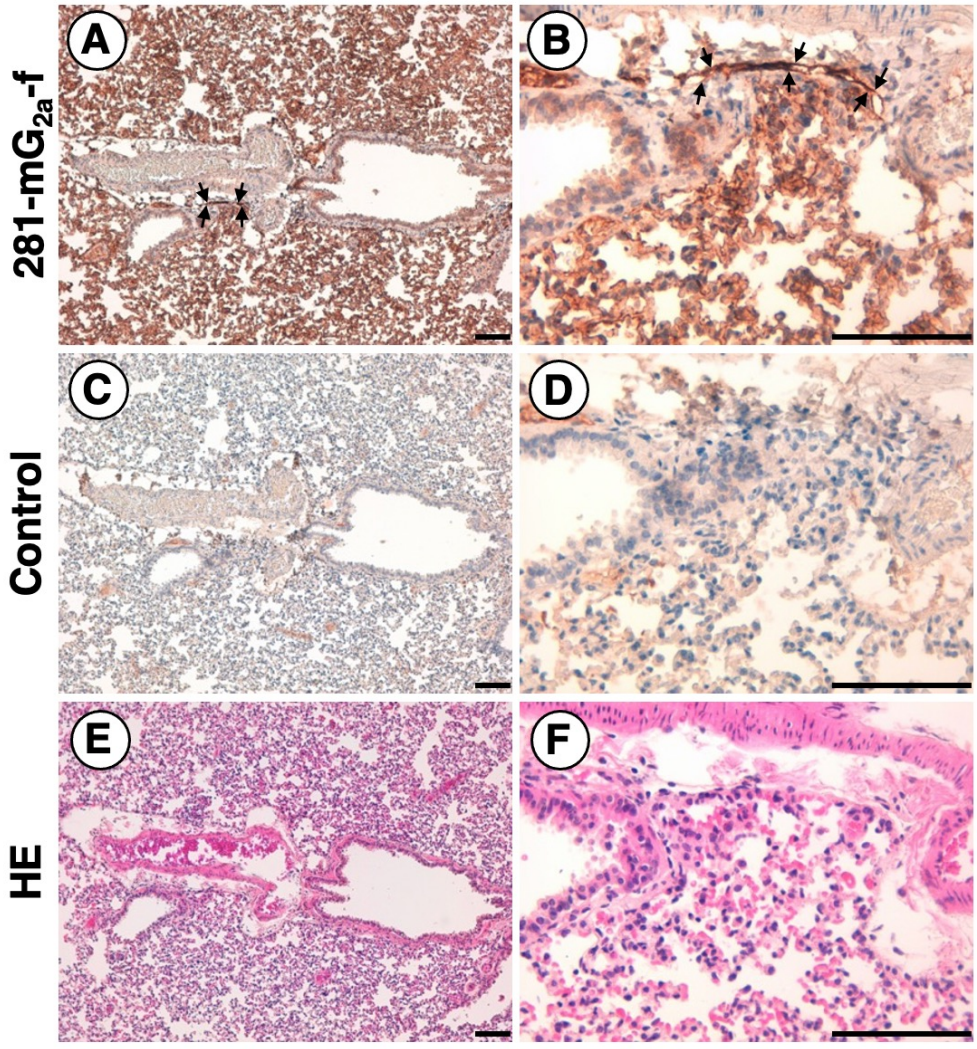

FIG. 5. Immunohistochemical analysis of golden hamster lung tissue. Histological sections of golden hamster lung were directly autoclaved in EnVision FLEX Target Retrieval Solution High pH and incubated with 5 µg/mL of 281-mG$_{2a}$-f **(A, B)** or blocking buffer **(C, D)**, followed by using the EnVision+ Kit. **(E, F)** H&E staining. Arrows show that PDPN is expressed in lymphatic endothelial cells. Scale bar = 100 µm. H&E, Hematoxylin and Eosin.

Results

Establishment of anti-ChamPDPN mAbs

To develop anti-ChamPDPN mAbs, the CBIS method, using stable transfectants for immunization and flow cytometry, was utilized (Fig. 1). A mouse was immunized with CHO/MAP-ChamPDPN cells, which overexpress ChamPDPN with an N-terminal MAP tag. Hybridomas were seeded into 96-well plates, and CHO/2 × RIEDL-ChamPDPN (hereinafter referred to as CHO/ChamPDPN)-positive and CHO-K1-negative wells were identified. After conducting limiting dilution and selection using immunohistochemistry, the PMab-281 (mouse IgG_3, kappa) was isolated.

The subclass of PMab-281 was converted from IgG_3 to IgG_{2a} because the mouse IgG_3 subclass is easy to aggregate. Additionally, a defucosylated anti-ChamPDPN mAb (281-mG_{2a}-f) was produced using BINDS-09 cells (FUT8-knocked out ExpiCHO-S cells). This process is summarized in Figure 2.

Flow cytometric analyses

Flow cytometric analyses were performed using 281-mG_{2a}-f with CHO/ChamPDPN and CHO-K1 cells. 281-mG_{2a}-f also recognized CHO/ChamPDPN but weakly reacted with CHO-K1 cells (Fig. 3A). In addition, 281-mG_{2a}-f cross-reacted with CHO/GhamPDPN, which overexpressed GhamPDPN (Fig. 3B). The 281-mG_{2a}-f also reacted with endogenous GhamPDPN, which is expressed in a golden hamster kidney cell line, BHK-21. These results showed that 281-mG_{2a}-f is suitable for detecting ChamPDPN and GhamPDPN using flow cytometry.

Kinetic analysis of 281-mG_{2a}-f interactions with CHO/ChamPDPN, CHO/GhamPDPN, and BHK-21 cells was conducted using flow cytometry. As indicated in Figure 4, the K_D for 281-mG_{2a}-f interactions with CHO/ChamPDPN, CHO/GhamPDPN, and BHK-21 cells was 5.0×10^{-9} M, 4.2×10^{-9} M, and 5.5×10^{-8} M, respectively, suggesting that 281-mG_{2a}-f exhibited a high affinity for both ChamPDPN and GhamPDPN.

Immunohistochemical analyses

To investigate whether 281-mG_{2a}-f can be used for immunohistochemical analyses using formalin-fixed paraffin-embedded (FFPE) golden hamster tissue sections, normal lung and kidney tissues from golden hamster were examined. Both of these reportedly express PDPN in different

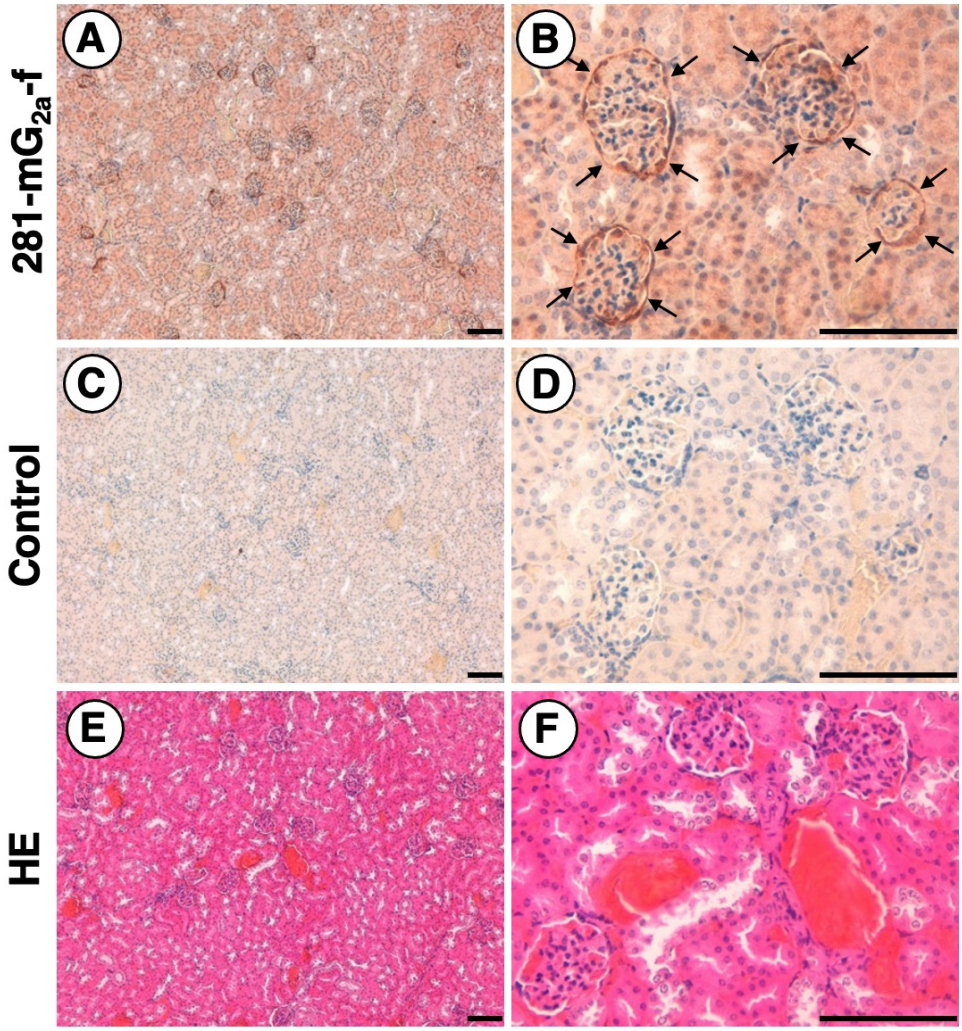

FIG. 6. Immunohistochemical analysis of golden hamster kidney tissue. Histological sections of the golden hamster kidney were directly autoclaved in EnVision FLEX Target Retrieval Solution High pH and incubated with 5 μg/mL of 281-mG_{2a}-f **(A, B)** or blocking buffer **(C, D)**, followed by the use of the EnVision+ Kit. **(E, F)** H&E staining. Arrows indicate that PDPN is expressed in Bowman's capsules. Scale bar = 100 μm.

species, including human,[20] mouse,[21] rat,[22] rabbit,[23] dog,[24] cat,[25] bovine,[26] pig,[27] Tasmanian devil,[28] alpaca,[29] tiger,[30] whale,[31] goat,[32] horse,[33] bears,[34] and sheep.[16,35] As indicated in Figure 5, 281-mG_{2a}-f strongly and specifically identified type I alveolar cells within the lung. Lymphatic endothelial cells of the lung were also detected using 281-mG_{2a}-f (Fig. 5). Additionally, 281-mG_{2a}-f identified Bowman's capsules in the kidney, but the glomerulus was weakly stained (Fig. 6). These results indicate that 281-mG_{2a}-f is useful for detecting GhamPDPN-positive cells in FFPE tissue.

Discussion

PMab-281 was originally developed as an anti-ChamPDPN mAb. In this study, we demonstrated that 281-mG_{2a}-f obtained from PMab-281, has strong cross-reactivity to GhamPDPN. The 281-mG_{2a}-f is available for flow cytometry (Fig. 3) and immunohistochemistry (Figs. 5 and 6). Compared with amino acid sequences between ChamPDPN and GhamPDPN, the identity is about 80%. Since the 281-mG_{2a}-f recognizes CHO/ChamPDPN and CHO/GhamPDPN cells with equivalent intensity (Fig. 3) and has a similar K_D value to both (Fig. 4), 281-mG_{2a}-f could recognize almost of the same epitope.

We have performed a conventional alanine-scanning method[16,36–57] for epitope mapping. We further developed the RIEDL insertion for epitope mapping (REMAP) method[58–61] for epitope mapping. The conformational epitopes of anti-EGFR mAbs (EMab-51 and EMab-134)[59,61] and anti-CD44 mAbs (C_{44}Mab-5 and C_{44}Mab-46)[58,60] could be determined using the REMAP method. Therefore, further studies are warranted for assessing the epitope of 281-mG_{2a}-f.

During the global pandemic of SARS-CoV-2, the golden hamster is in the spotlight as an animal model owing to its similarity with human pathogenesis.[62] Currently, the golden hamster is mainly used as a mild SARS-CoV-2 infection model.[8,63] SARS-CoV-2-inoculated animals consistently lose their body weight during the first week of infection. After a week, when the infectious virus was cleared, interstitial and alveolar macrophage infiltrates and marked reparative epithelial hyperplasia dominated in the lung. At terminal time points, enhanced lung weights and developed lung consolidation were observed. The use of 281-mG_{2a}-f to investigate the morphologic alterations in lung type I alveolar epithelial cells could provide valuable pathogenesis information and develop therapeutic measures against SARS-CoV-2.

SARS-CoV-2 can lead to severe sepsis and systemic inflammation in human patients, which induce multiple organ dysfunctions.[64] Among them, acute kidney injury is predictive of mortality in the patients. Beyond the cytokine storm and hemodynamic instability, SARS-CoV-2 might directly cause kidney injury, including acute tubular necrosis, podocytopathy (podocyte injury), and microangiopathy in the glomeruli. Francis *et al.* reported kidney histology in SARS-CoV-2-infected golden hamsters and observed acute tubular inflammation and injury.[65] Although PDPN is known to be expressed in kidney podocytes,[3] the reactivity of 281-mG_{2a}-f to kidney podocytes was weak (Fig. 6). Further studies are required to confirm the reactivity of 281-mG_{2a}-f in the kidney. The 281-mG_{2a}-f might contribute to the analysis of kidney injury in SARS-CoV-2-infected animals.

Author Disclosure Statement

No competing financial interests exist.

Funding Information

This research was supported in part by Japan Agency for Medical Research and Development (AMED) under Grant Numbers: JP22ama121008 (to Y.K.), JP21am0401013 (to Y.K.), and JP21am0101078 (to Y.K.), and by the Japan Society for the Promotion of Science (JSPS) Grants-in-Aid for Scientific Research (KAKENHI) Grant Nos. 21K06059 (to M. Saito), 20K16322 (M. Sano), 21K20789 (to T.T.), 21K15523 (to T.A.), 21K07168 (to M.K.K.), and 19K07705 (to Y.K.).

References

1. Dobbs LG, Williams MC, and Gonzalez R: Monoclonal antibodies specific to apical surfaces of rat alveolar type I cells bind to surfaces of cultured, but not freshly isolated, type II cells. Biochim Biophys Acta 1988;970:146–156.
2. Rishi AK, Joyce-Brady M, Fisher J, Dobbs LG, Floros J, VanderSpek J, Brody JS, and Williams MC: Cloning, characterization, and development expression of a rat lung alveolar type I cell gene in embryonic endodermal and neural derivatives. Dev Biol 1995;167:294–306.
3. Breiteneder-Geleff S, Matsui K, Soleiman A, Meraner P, Poczewski H, Kalt R, Schaffner G, and Kerjaschki D: Podoplanin, novel 43-kd membrane protein of glomerular epithelial cells, is down-regulated in puromycin nephrosis. Am J Pathol 1997;151:1141–1152.
4. Garg P: A review of podocyte biology. Am J Nephrol 2018; 47 Suppl 1:3–13.
5. Hirakawa S, Hong YK, Harvey N, Schacht V, Matsuda K, Libermann T, and Detmar M: Identification of vascular lineage-specific genes by transcriptional profiling of isolated blood vascular and lymphatic endothelial cells. Am J Pathol 2003;162:575–586.
6. Petrova TV, Mäkinen T, Mäkelä TP, Saarela J, Virtanen I, Ferrell RE, Finegold DN, Kerjaschki D, Ylä-Herttuala S, and Alitalo K: Lymphatic endothelial reprogramming of vascular endothelial cells by the Prox-1 homeobox transcription factor. EMBO J 2002;21:4593–4599.
7. Schacht V, Ramirez MI, Hong YK, Hirakawa S, Feng D, Harvey N, Williams M, Dvorak AM, Dvorak HF, Oliver G, and Detmar M: T1alpha/podoplanin deficiency disrupts normal lymphatic vasculature formation and causes lymphedema. EMBO J 2003;22:3546–3556.
8. Sia SF, Yan LM, Chin AWH, Fung K, Choy KT, Wong AYL, Kaewpreedee P, Perera R, Poon LLM, Nicholls JM, Peiris M, and Yen HL: Pathogenesis and transmission of SARS-CoV-2 in golden hamsters. Nature 2020;583:834–838.
9. Kreye J, Reincke SM, Kornau HC, Sánchez-Sendin E, Corman VM, Liu H, Yuan M, Wu NC, Zhu X, Lee CD, Trimpert J, Höltje M, Dietert K, Stöffler L, von Wardenburg N, van Hoof S, Homeyer MA, Hoffmann J, Abdelgawad A, Gruber AD, Bertzbach LD, Vladimirova D, Li LY, Barthel PC, Skriner K, Hocke AC, Hippenstiel S, Witzenrath M, Suttorp N, Kurth F, Franke C, Endres M, Schmitz D, Jeworowski LM, Richter A, Schmidt ML, Schwarz T, Müller MA, Drosten C, Wendisch D, Sander LE, Osterrieder N, Wilson IA, and Prüss H: A therapeutic non-self-reactive SARS-CoV-2 antibody protects from lung pathology in a COVID-19 Hamster Model. Cell 2020;183: 1058–1069.e1019.

10. Fujii Y, Kaneko MK, and Kato Y: MAP Tag: A novel tagging system for protein purification and detection. Monoclon Antib Immunodiagn Immunother 2016;35:293–299.
11. Wakasa A, Kaneko MK, Kato Y, Takagi J, and Arimori T: Site-specific epitope insertion into recombinant proteins using the MAP tag system. J Biochem 2020;168:375–384.
12. Asano T, Kaneko MK, and Kato Y: RIEDL tag: A novel pentapeptide tagging system for transmembrane protein purification. Biochem Biophys Rep 2020;23:100780.
13. Itai S, Fujii Y, Nakamura T, Chang YW, Yanaka M, Saidoh N, Handa S, Suzuki H, Harada H, Yamada S, Kaneko MK, and Kato Y: Establishment of CMab-43, a sensitive and specific anti-CD133 monoclonal antibody, for immunohistochemistry. Monoclon Antib Immunodiagn Immunother 2017;36:231–235.
14. Furusawa Y, Kaneko MK, and Kato Y: Establishment of an anti-CD20 monoclonal antibody (C(20)Mab-60) for immunohistochemical analyses. Monoclon Antib Immunodiagn Immunother 2020;39:112–116.
15. Furusawa Y, Kaneko MK, and Kato Y: Establishment of C(20)Mab-11, a novel anti-CD20 monoclonal antibody, for the detection of B cells. Oncol Lett 2020;20:1961–1967.
16. Kaneko MK, Sano M, Takei J, Asano T, Sayama Y, Hosono H, Kobayashi A, Konnai S, and Kato Y: Development and characterization of anti-sheep podoplanin monoclonal antibodies PMab-253 and PMab-260. Monoclon Antib Immunodiagn Immunother 2020;39:144–155.
17. Tanaka T, Asano T, Sano M, Takei J, Hosono H, Nanamiya R, Nakamura T, Yanaka M, Harada H, Fukui M, Suzuki H, Uchida K, Nakagawa T, Kato Y, and Kaneko MK: Development of monoclonal antibody PMab-269 against california sea lion podoplanin. Monoclon Antib Immunodiagn Immunother 2021;40:124–133.
18. Yamada S, Itai S, Nakamura T, Yanaka M, Chang YW, Suzuki H, Kaneko MK, and Kato Y: Monoclonal antibody L1Mab-13 detected human PD-L1 in lung cancers. Monoclon Antib Immunodiagn Immunother 2018;37:110–115.
19. Yamada S, Itai S, Nakamura T, Yanaka M, Kaneko MK, and Kato Y: Detection of high CD44 expression in oral cancers using the novel monoclonal antibody, C44Mab-5. Biochem Biophys Rep 2018;14:64–68.
20. Kato Y, Kaneko MK, Kuno A, Uchiyama N, Amano K, Chiba Y, Hasegawa Y, Hirabayashi J, Narimatsu H, Mishima K, and Osawa M: Inhibition of tumor cell-induced platelet aggregation using a novel anti-podoplanin antibody reacting with its platelet-aggregation-stimulating domain. Biochem Biophys Res Commun 2006;349:1301–1307.
21. Kaji C, Tsujimoto Y, Kato Kaneko M, Kato Y, and Sawa Y: Immunohistochemical examination of novel rat monoclonal antibodies against mouse and human podoplanin. Acta Histochem Cytochem 2012;45:227–237.
22. Oki H, Honma R, Ogasawara S, Fujii Y, Liu X, Takagi M, Kaneko MK, and Kato Y: Development of sensitive monoclonal antibody PMab-2 against rat podoplanin. Monoclon Antib Immunodiagn Immunother 2015;34:396–403.
23. Honma R, Fujii Y, Ogasawara S, Oki H, Liu X, Nakamura T, Kaneko MK, Takagi M, and Kato Y: Establishment of a novel monoclonal antibody PMab-32 against rabbit podoplanin. Monoclon Antib Immunodiagn Immunother 2016;35:41–47.
24. Honma R, Kaneko MK, Ogasawara S, Fujii Y, Konnai S, Takagi M, and Kato Y: Specific detection of dog podoplanin expressed in renal glomerulus by a novel monoclonal antibody PMab-38 in immunohistochemistry. Monoclon Antib Immunodiagn Immunother 2016;35:212–216.
25. Yamada S, Itai S, Nakamura T, Yanaka M, Saidoh N, Chang YW, Handa S, Harada H, Kagawa Y, Ichii O, Konnai S, Kaneko MK, and Kato Y: PMab-52: Specific and sensitive monoclonal antibody against cat podoplanin for immunohistochemistry. Monoclon Antib Immunodiagn Immunother 2017;36:224–230.
26. Honma R, Ogasawara S, Kaneko M, Fujii Y, Oki H, Nakamura T, Takagi M, Konnai S, and Kato Y: PMab-44 detects bovine podoplanin in immunohistochemistry. Monoclon Antib Immunodiagn Immunother 2016;35:186–190.
27. Kato Y, Yamada S, Furusawa Y, Itai S, Nakamura T, Yanaka M, Sano M, Harada H, Fukui M, and Kaneko MK: PMab-213: A monoclonal antibody for immunohistochemical analysis against pig podoplanin. Monoclon Antib Immunodiagn Immunother 2019;38:18–24.
28. Furusawa Y, Yamada S, Itai S, Nakamura T, Takei J, Sano M, Harada H, Fukui M, Kaneko MK, and Kato Y: Establishment of a monoclonal antibody PMab-233 for immunohistochemical analysis against Tasmanian devil podoplanin. Biochem Biophys Rep 2019;18:100631.
29. Kato Y, Furusawa Y, Yamada S, Itai S, Takei J, Sano M, and Kaneko MK: Establishment of a monoclonal antibody PMab-225 against alpaca podoplanin for immunohistochemical analyses. Biochem Biophys Rep 2019;18:100633.
30. Furusawa Y, Kaneko MK, Nakamura T, Itai S, Fukui M, Harada H, Yamada S, and Kato Y: Establishment of a monoclonal antibody PMab-231 for tiger podoplanin. Monoclon Antib Immunodiagn Immunother 2019;38:89–95.
31. Kato Y, Furusawa Y, Itai S, Takei J, Nakamura T, Sano M, Harada H, Yamada S, and Kaneko MK: Establishment of an anticetacean podoplanin monoclonal antibody PMab-237 for immunohistochemical analysis. Monoclon Antib Immunodiagn Immunother 2019;38:108–113.
32. Furusawa Y, Yamada S, Nakamura T, Sano M, Sayama Y, Itai S, Takei J, Harada H, Fukui M, Kaneko MK, and Kato Y: PMab-235: A monoclonal antibody for immunohistochemical analysis against goat podoplanin. Heliyon 2019;5:e02063.
33. Furusawa Y, Yamada S, Itai S, Sano M, Nakamura T, Yanaka M, Handa S, Mizuno T, Maeda K, Fukui M, Harada H, Kaneko MK, and Kato Y: Establishment of monoclonal antibody PMab-202 against horse podoplanin. Monoclon Antib Immunodiagn Immunother 2018;37:233–237.
34. Takei J, Furusawa Y, Yamada S, Nakamura T, Sayama Y, Sano M, Konnai S, Kobayashi A, Harada H, Kaneko MK, and Kato Y: PMab-247 detects bear podoplanin in immunohistochemical analysis. Monoclon Antib Immunodiagn Immunother 2019;38:171–174.
35. Kato Y, Furusawa Y, Sano M, Takei J, Nakamura T, Yanaka M, Okamoto S, Handa S, Komatsu Y, Asano T, Sayama Y, and Kaneko MK: Development of an anti-sheep podoplanin monoclonal antibody PMab-256 for immunohistochemical analysis of lymphatic endothelial cells. Monoclon Antib Immunodiagn Immunother 2020;39:82–90.
36. Chang YW, Kaneko MK, Yamada S, and Kato Y: Epitope mapping of monoclonal antibody PMab-52 against cat

podoplanin. Monoclon Antib Immunodiagn Immunother 2018;37:95–99.
37. Chang YW, Yamada S, Kaneko MK, and Kato Y: Epitope mapping of monoclonal antibody PMab-38 against dog podoplanin. Monoclon Antib Immunodiagn Immunother 2017;36:291–295.
38. Furusawa Y, Yamada S, Itai S, Nakamura T, Fukui M, Harada H, Kaneko MK, and Kato Y: Elucidation of critical epitope of anti-rat podoplanin monoclonal antibody PMab-2. Monoclon Antib Immunodiagn Immunother 2018;37:188–193.
39. Honma R, Fujii Y, Ogasawara S, Oki H, Konnai S, Kagawa Y, Takagi M, Kaneko MK, and Kato Y: critical epitope of anti-rabbit podoplanin monoclonal antibodies for immunohistochemical analysis. Monoclon Antib Immunodiagn Immunother 2016;35:65–72.
40. Kaneko MK, Furusawa Y, Sano M, Itai S, Takei J, Harada H, Fukui M, Yamada S, and Kato Y: Epitope mapping of the antihorse podoplanin monoclonal antibody PMab-202. Monoclon Antib Immunodiagn Immunother 2019;38:79–84.
41. Kaneko MK, Nakamura T, Kunita A, Fukayama M, Abe S, Nishioka Y, Yamada S, Yanaka M, Saidoh N, Yoshida K, Fujii Y, Ogasawara S, and Kato Y: ChLpMab-23: Cancer-specific human-mouse chimeric anti-podoplanin antibody exhibits antitumor activity via antibody-dependent cellular cytotoxicity. Monoclon Antib Immunodiagn Immunother 2017;36:104–112.
42. Kaneko MK, Oki H, Hozumi Y, Liu X, Ogasawara S, Takagi M, Goto K, and Kato Y: Monoclonal antibody LpMab-9 recognizes O-glycosylated N-terminus of human podoplanin. Monoclon Antib Immunodiagn Immunother 2015;34:310–317.
43. Kaneko MK, Yamada S, Itai S, Chang YW, Nakamura T, Yanaka M, and Kato Y: Elucidation of the critical epitope of an anti-EGFR monoclonal antibody EMab-134. Biochem Biophys Rep 2018;14:54–57.
44. Kato Y, Kunita A, Fukayama M, Abe S, Nishioka Y, Uchida H, Tahara H, Yamada S, Yanaka M, Nakamura T, Saidoh N, Yoshida K, Fujii Y, Honma R, Takagi M, Ogasawara S, Murata T, and Kaneko MK: Antiglycopeptide mouse monoclonal antibody LpMab-21 exerts antitumor activity against human podoplanin through antibody-dependent cellular cytotoxicity and complement-dependent cytotoxicity. Monoclon Antib Immunodiagn Immunother 2017;36:20–24.
45. Kato Y, Ogasawara S, Oki H, Goichberg P, Honma R, Fujii Y, and Kaneko MK: LpMab-12 Established by CasMab technology specifically detects sialylated O-glycan on Thr52 of platelet aggregation-stimulating domain of human podoplanin. PLoS One 2016;11:e0152912.
46. Kato Y, Sayama Y, Sano M, and Kaneko MK: Epitope analysis of an antihorse podoplanin monoclonal antibody PMab-219. Monoclon Antib Immunodiagn Immunother 2019;38:266–270.
47. Kato Y, Takei J, Furusawa Y, Sayama Y, Sano M, Konnai S, Kobayashi A, Harada H, Takahashi M, Suzuki H, Yamada S, and Kaneko MK: Epitope mapping of anti-bear podoplanin monoclonal antibody PMab-247. Monoclon Antib Immunodiagn Immunother 2019;38:230–233.
48. Sano M, Kaneko MK, and Kato Y: Epitope mapping of monoclonal antibody PMab-233 against tasmanian devil podoplanin. Monoclon Antib Immunodiagn Immunother 2019;38:261–265.
49. Sayama Y, Sano M, Asano T, Furusawa Y, Takei J, Nakamura T, Yanaka M, Okamoto S, Handa S, Komatsu Y, Nakamura Y, Yanagawa M, Kaneko MK, and Kato Y: Epitope mapping of PMab-241, a lymphatic endothelial cell-specific anti-bear podoplanin monoclonal antibody. Monoclon Antib Immunodiagn Immunother 2020;39:77–81.
50. Sayama Y, Sano M, Furusawa Y, Kaneko MK, and Kato Y: Epitope mapping of PMab-225 an anti-alpaca podoplanin monoclonal antibody using flow cytometry. Monoclon Antib Immunodiagn Immunother 2019;38:255–260.
51. Sayama Y, Sano M, Kaneko MK, and Kato Y: Epitope analysis of an anti-whale podoplanin monoclonal antibody, PMab-237, using flow cytometry. Monoclon Antib Immunodiagn Immunother 2020;39:17–22.
52. Takei J, Itai S, Furusawa Y, Yamada S, Nakamura T, Sano M, Harada H, Fukui M, Kaneko MK, and Kato Y: Epitope mapping of anti-tiger podoplanin monoclonal antibody PMab-231. Monoclon Antib Immunodiagn Immunother 2019;38:129–132.
53. Tanaka T, Asano T, Sano M, Takei J, Hosono H, Nanamiya R, Tateyama N, Kaneko MK, and Kato Y: Epitope mapping of the anti-california sea lion podoplanin monoclonal antibody PMab-269 using alanine-scanning mutagenesis and ELISA. Monoclon Antib Immunodiagn Immunother 2021;40:196–200.
54. Yamada S, Itai S, Furusawa Y, Kaneko MK, and Kato Y: Epitope mapping of antipig podoplanin monoclonal antibody PMab-213. Monoclon Antib Immunodiagn Immunother 2019;38:224–229.
55. Yamada S, Itai S, Kaneko MK, Konnai S, and Kato Y: Epitope mapping of anti-mouse podoplanin monoclonal antibody PMab-1. Biochem Biophys Rep 2018;15:52–56.
56. Yamada S, Kaneko MK, Itai S, Chang YW, Nakamura T, Yanaka M, Ogasawara S, Murata T, Uchida H, Tahara H, Harada H, and Kato Y: Epitope mapping of monoclonal antibody PMab-48 against dog podoplanin. Monoclon Antib Immunodiagn Immunother 2018;37:162–165.
57. Takei J, Asano T, Suzuki H, Kaneko MK, and Kato Y: Epitope Mapping of the Anti-CD44 Monoclonal antibody (C44Mab-46) using alanine-scanning mutagenesis and surface plasmon resonance. Monoclon Antib Immunodiagn Immunother 2021;40:219–226.
58. Asano T, Kaneko MK, Takei J, Tateyama N, and Kato Y: Epitope mapping of the anti-CD44 monoclonal antibody (C44Mab-46) using the REMAP Method. Monoclon Antib Immunodiagn Immunother 2021;40:156–161.
59. Sano M, Kaneko MK, Aasano T, and Kato Y: Epitope mapping of an antihuman EGFR monoclonal antibody (EMab-134) using the REMAP Method. Monoclon Antib Immunodiagn Immunother 2021;40:191–195.
60. Asano T, Kaneko MK, and Kato Y: Development of a novel epitope mapping system: RIEDL insertion for Epitope Mapping Method. Monoclon Antib Immunodiagn Immunother 2021;40:162–167.
61. Nanamiya R, Sano M, Asano T, Yanaka M, Nakamura T, Saito M, Tanaka T, Hosono H, Tateyama N, Kaneko MK, and Kato Y: Epitope mapping of an anti-human epidermal growth factor receptor monoclonal antibody (EMab-51) using the RIEDL Insertion for Epitope Mapping Method. Monoclon Antib Immunodiagn Immunother 2021;40:149–155.

62. Muñoz-Fontela C, Dowling WE, Funnell SGP, Gsell PS, Riveros-Balta AX, Albrecht RA, Andersen H, Baric RS, Carroll MW, Cavaleri M, Qin C, Crozier I, Dallmeier K, de Waal L, de Wit E, Delang L, Dohm E, Duprex WP, Falzarano D, Finch CL, Frieman MB, Graham BS, Gralinski LE, Guilfoyle K, Haagmans BL, Hamilton GA, Hartman AL, Herfst S, Kaptein SJF, Klimstra WB, Knezevic I, Krause PR, Kuhn JH, Le Grand R, Lewis MG, Liu WC, Maisonnasse P, McElroy AK, Munster V, Oreshkova N, Rasmussen AL, Rocha-Pereira J, Rockx B, Rodríguez E, Rogers TF, Salguero FJ, Schotsaert M, Stittelaar KJ, Thibaut HJ, Tseng CT, Vergara-Alert J, Beer M, Brasel T, Chan JFW, García-Sastre A, Neyts J, Perlman S, Reed DS, Richt JA, Roy CJ, Segalés J, Vasan SS, Henao-Restrepo AM, and Barouch DH: Animal models for COVID-19. Nature 2020;586:509–515.
63. Mulka KR, Beck SE, Solis CV, Johanson AL, Queen SE, McCarron ME, Richardson MR, Zhou R, Marinho P, Jedlicka A, Guerrero-Martin S, Shirk EN, Braxton AM, Brockhurst J, Creisher PS, Dhakal S, Brayton CF, Veenhuis RT, Metcalf Pate KA, Karakousis PC, Zahnow CA, Klein SL, Jain SK, Tarwater PM, Pekosz AS, Villano JS, and Mankowski JL: Progression and resolution of SARS-CoV-2 infection in golden syrian hamsters. Am J Pathol 2021;192:195–207.
64. Chueh TI, Zheng CM, Hou YC, and Lu KC: Novel evidence of acute kidney injury in COVID-19. J Clin Med 2020;9:3547.
65. Francis ME, Goncin U, Kroeker A, Swan C, Ralph R, Lu Y, Etzioni AL, Falzarano D, Gerdts V, Machtaler S, Kindrachuk J, and Kelvin AA: SARS-CoV-2 infection in the Syrian hamster model causes inflammation as well as type I interferon dysregulation in both respiratory and non-respiratory tissues including the heart and kidney. PLoS Pathog 2021;17:e1009705.

Address correspondence to:
Yukinari Kato
Department of Molecular Pharmacology
Tohoku University Graduate School of Medicine
2-1, Seiryo-machi, Aoba-ku
Sendai
Miyagi 980-8575
Japan

E-mail: yukinarikato@med.tohoku.ac.jp

Received: November 21, 2021
Accepted: February 14, 2022